Journal of Archaeological Science: Reports 33 (2020) 102553

Contents lists available at ScienceDirect

Journal of Archaeological Science: Reports

journal homepage: www.elsevier.com/locate/jasrep

# A new method for the identification of archaeological soils by their spectral signatures in the vis-NIR region

Y.J. Choi[a,*,1], J. Lampel[a,b,2], S. Fiedler[c], D. Jordan[d], T. Wagner[a]

[a] Max Planck Institute for Chemistry, Hahn-Meitner-Weg 1, 55128 Mainz, Germany
[b] Institute of Environmental Physics, University of Heidelberg, Heidelberg, and Airyx GmbH, Eppelheim, Germany
[c] Institute of Geography, Johannes Gutenberg University, Johann-Joachim-Becher-Weg 21, 55099 Mainz, Germany
[d] School of Biological and Environmental Sciences, Liverpool John Moores University, Liverpool, UK

ARTICLE INFO

*Keywords:*
Soil spectra
PCA
Archaeological prospection
vis-NIR reflectance spectra

ABSTRACT

This paper introduces a statistical method to identify spectral signatures of buried archaeological remains and distinguish them from spectra of the background soil in the visible to near infrared region. The proposed method is based on the Principal Component Analysis (PCA). The difference between an archaeological spectrum and non-archaeological soil spectra is quantified by a so-called R value. R values larger than 1 indicate that the spectrum represents an archaeological material. The method is successfully applied to samples from five study sites in Italy and Hungary with special conditions. The reflection spectra are taken in a time-efficient way with a field spectrometer. The method works best if background non-archaeological soil spectra are gathered from the same area, around the targeted archaeological site. Also, it can work without such local background spectra (but with lower accuracy) using background spectra from existing spectral libraries. This indicates that the method can, in principle, be applied to any archaeological site which is spectrally distinct from its surroundings. The paper highlights that this method does not require high spectral resolution and thus has the advantage of using low spectral resolution spectrometers which can eventually be applied for continuous 2D imaging applications with high temporal resolution. Additional studies are needed to further improve the method and to investigate under which conditions it works well or only with limited accuracy.

## 1. Introduction

Buried archaeological remains tend to be different from the adjacent soil. Visible to near infrared spectroscopic techniques can be a useful tool to analyze not only soil compounds but also soil properties, since they are indicative, rapid, non-destructive and low-cost analytical methods. They also stand out as among the few methods which can make use of an airborne or space-borne platform so that data can, at least in principle, be gathered very rapidly at high spatial resolution. Therefore, soil spectroscopy has been widely used to investigate various soil properties (Ben-Dor and Banin, 1995; Clark et al., 1990, 2003; Viscarra Rossel et al., 2011; Wetterlind et al., 2013), such as soil organic matter (Hong et al., 2018), moisture content (Ben-Dor et al., 2008; Liu et al., 2003), soil texture (Stenberg et al., 2010). Also, soil compounds such as carbonates (Stenberg et al., 2010), clay minerals (Stenberg et al., 2010; Viscarra Rossel et al., 2011), and metals/metalloids (Ben Dor et al., 1999; Nocita et al, 2015) are also detectable using soil spectra. In many soils, especially those of warm climates and oxidizing soil environments, the visible range of the soil spectra is mainly sensitive to the presence of ferrous and ferric iron oxides, and the electronic transition of the iron cations (Ben-Dor et al., 1997). In cooler and wetter regions, where the soil environment is often less biologically active and less oxidizing, organic matter can accumulate and soil spectra are also strongly affected by absorption by these organic components (Angelopoulou et al., 2019). Ben-Dor et al. (2002), Viscarra Rossel and Behrens (2010), and Soriano-Disla et al. (2014) have published tables of absorption positions of soil spectra and the related soil components.

Spectroscopic analysis of archaeological soils can provide useful information of the soil properties, but the link between soil chemistry, soil physics and archaeology is usually complex and not yet well understood (Oonk et al., 2009). In geochemical studies, archaeological soils have been analyzed with respect to the contents of certain

* Corresponding author.
*E-mail addresses:* y.choi@mpic.de, yoonjung.choi06@gmail.com, depicu@gmail.com (Y.J. Choi).
[1] Now at: Seoul National University Museum, Seoul, Republic of Korea.
[2] Now at: Airyx GmbH, Eppelheim, Germany.

https://doi.org/10.1016/j.jasrep.2020.102553
Received 5 April 2020; Received in revised form 17 August 2020; Accepted 26 August 2020

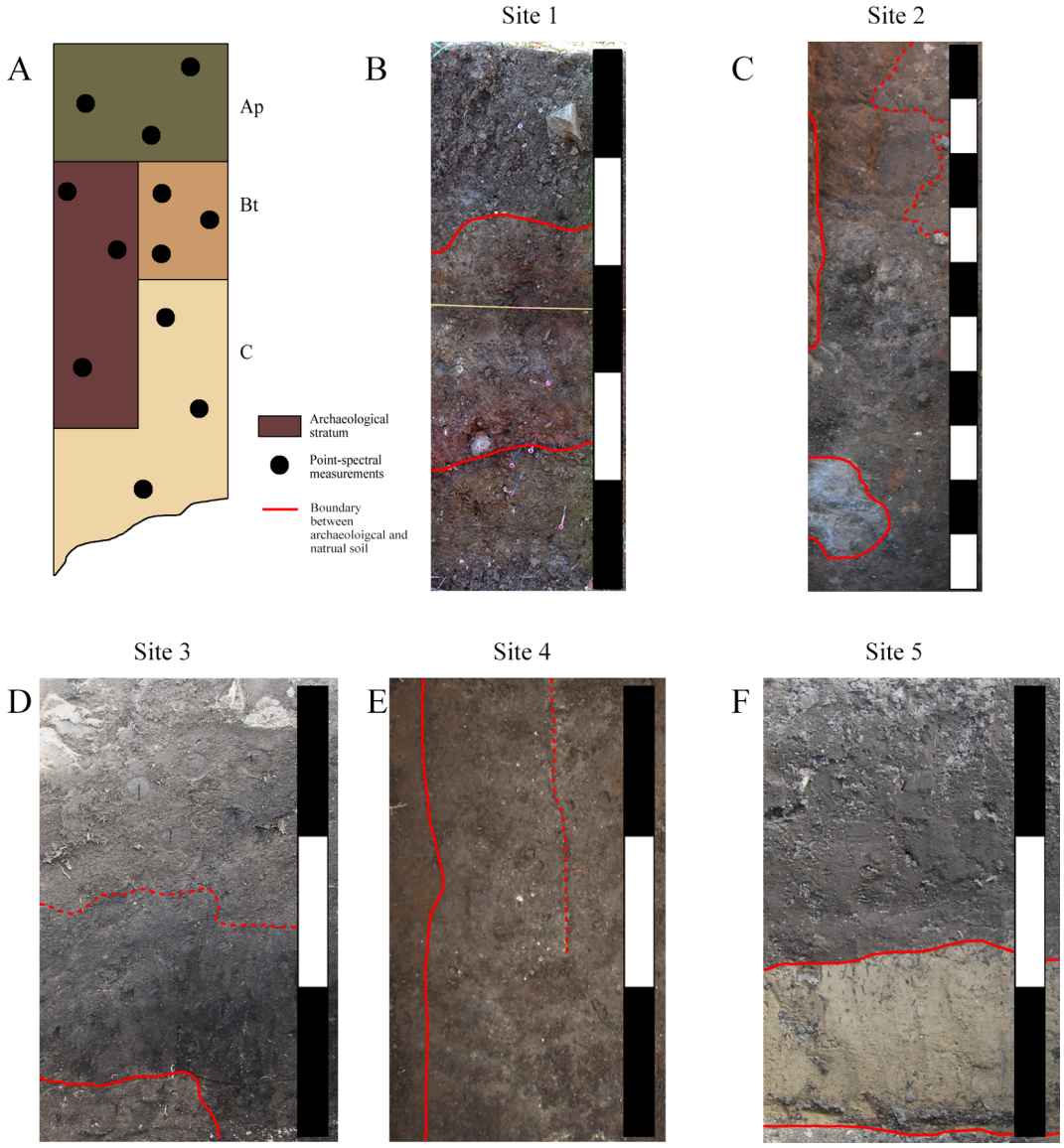


**Fig. 1.** Schematic image (A) and photos (B to F) of soil profiles including archaeological features. The depth of most of the pits is approximately 1 m, below which the parent soil is observed. At least three point spectral measurements were taken at each soil horizon with the ASD contact probe. The selected archaeological sites are located on arable land and, therefore, they contain Ap horizons. Images B, D and F are soil profile including an archaeological stratum (red, black and yellow layer respectively). Images C and E are floor of the excavated archaeological pit at 100 cm and 60 cm depth. Each step on the scale bar corresponds to 20 cm.

elements (Oonk et al., 2009). For example, Ca, Cu, Mg, K, Na, P and Zn are sometimes found in archaeological soils in high concentrations (Cook and Heizer, 1964; Eidt, 1984; Haslam and Tibbett, 2004; Middleton and Price, 1996; Ottaway and Matthews, 1988), since these elements are often present in occupation waste (Greweling, 1962; Hao and Chang, 2003; Maly et al., 1999). Element abundance is often related to distinct functional area but many of these elements may not be found uniformly in different archaeological soils (Oonk et al., 2009).

In archaeology, vis-NIR spectroscopy has mostly been used to further enhance remote sensing capabilities (Grøn et al., 2011, Schmid et al., 2008). There have, to date, been only a few archaeological soil spectroscopy studies, even fewer using field spectrometers. For example, Buck et al. (2003) used vis-NIR spectra to identify pottery and showed that the concentration of pottery materials needed to be 85% or greater to be detected against background soils. Eckmeier and Gerlach (2012) compared the charred organic matter concentration to soil color using visible spectra and showed that charred organic matter influenced soil color more than total soil organic matter for pit fillings. Matney et al. (2014) presented *in-situ* subsurface reflectance spectroscopy of archaeological sites as tomographic maps. Araújo et al. (2015) used NIR spectra to study Amazonian Dark Earths to predict soil properties. Linderholm et al. (2019) used NIR spectra on archaeological soil profiles to understand site development and soil formation. Despite the various use of vis–NIR spectra, the identification of archaeological soil horizons using the field spectrometer has not been studied widely yet.

In this paper, instead of analyzing the specific chemical properties of the soils and archaeological materials from the reflectance spectra, the whole spectral range is used to identify specific spectral signatures representing archeological materials. The objective of our study is to test a new statistical methodology to identify buried archaeological remains using hand-held spectrometers. This method is based on the principal component analysis (PCA) and, thus, identifies any 'unusual' spectral behavior (in this case archaeological spectra) within the dataset. To accomplish this, reflectance spectra of the archaeological remains and the surrounding soils are gathered during the excavation by a field spectrometer to develop and verify this methodology. Here, the soils from the archaeological strata are referred as 'archaeological soil'. The surrounding background soils, which are the 'non-archaeological'

soils, are referred to as 'natural soils' to distinguish them from the archaeological materials in which we are interested.

This method is non-destructive and quantitatively calculates specific values for any soil spectrum, which describes the probability of the tested material to be of anomalous anthropogenic, including archaeological origin. Thus, it can be used to identify archaeological strata quickly and it has the potential to be applied to airborne images in order to prospect for archaeological soil marks.

## 2. Material and methods

### 2.1. Study sites

Measurements were taken at five archaeological sites located on arable land where two sites are located in Calabria, Italy, and three sites are located in the Sárvíz Valley, Hungary. These sites were chosen to test the method in two contrasting environments. The two sites in Italy (sites 1 and 2) are located in the Raganello Valley catchment. The area is characterized by intensive tectonic activity and a Mediterranean climate modified by the topography which ranges from lowland valley to high, rocky mountains. As a result, the soils and geology are very complex. The Hungarian sites (sites 3, 4 and 5) are located on the Great Hungarian Plain, a flat and relatively homogeneous landscape mainly covered by a thick layer of loess. The buried remains in all of the study sites showed clear color differences compared to the surrounding materials. Both sites 1 and 2 (Italy) contain traces of prehistoric kitchen deposits with strong reddish archaeological strata including ceramic pieces and burned soil materials (Fig. 1B and C). Sites 3 and 5 are ditch formations, each filled with fallen wall fragments (Fig. 1D) and yellowish Hungarian loess (Fig. 1F), respectively. Site 4 is a pit feature interpreted as an ancient rubbish dump, which contained a high fraction of organic matter and, thus, has darker soil color than the surrounding soil (Fig. 1E). For every archaeological site, several soil pits (five soil pits for sites 1 and 2, and two soil pits for sites 3 to 5) were excavated around the site to collect background natural (non-archaeological) soil spectra.

### 2.2. Laboratory soil analysis

Soil samples were collected from each archaeological site for laboratory analysis. These samples were air dried and sieved to a size fraction $< 2$ mm. The soil samples were homogenized through grinding to analyze total carbon and nitrogen by dry combustion with an Elementar Vario EL cube (Elementar, Germany). The soil pH value was measured using filtrate of 10 g soil in 25 ml $CaCl_2$ (Van Reeuwijk, 2002) using glass electrodes (Minitrode, Hamilton Messetechnik GmbH, Höchst, Germany). The soil textural classes were estimated by a field estimation based on feeling the constituents of the soil (Jahn et al., 2006). When the soil samples ($< 2$ mm) are in wet state, the constituents have the following feel: Clay is sticky and formable whereas silt is smooth, non-sticky and only weakly formable. Sand cannot be formed and feels grainy (Jahn et al., 2006).

### 2.3. Spectrometer

Reflectance spectra were measured during the archaeological excavations using an ASD (Analytical Spectral Devices) FieldSpec Pro FR handheld spectrometer (Malvern Panalytical, Malvern, UK) which covers wavelengths from 350 to 2500 nm with a spectral sampling interval of 1 nm. This spectrometer is composed of three internal spectrometers where each spectrometer covers wavelength ranges of 350 – 1000 nm, 1000 – 1830 nm and 1830 – 2500 nm with spectral resolutions of 3, 10 and 12 nm, respectively. However, this paper only uses the wavelength range from 400 to 1000 nm since preliminary sensitivity studies indicated that most of the characteristic spectral information of the archaeological materials obtained in this study is found within this spectral range (Choi et al., 2015; Choi, 2018). Moreover, this range avoids the strong water absorption features in soil spectra around 1400, 1900 and 2200 nm range (Choi et al., 2015; Choi, 2018). To measure the *in-situ* soil spectra, an ASD Contact Probe attachment with an artificial halogen light source was used to illuminate the soil surface with a spot size of 10 mm.

### 2.4. Collection of the spectral dataset

Soil spectra were measured at different depths in a soil profile, extending from the surface (Ap horizon) to the bottom of the pit (C horizon, approximately 1 m depth) (Viscarra Rossel et al., 2009). For each point measurement of a soil horizon, the ASD spectrometer automatically measures and averages 35 spectra to improve the signal to noise ratio. Fig. 1A shows a schematic image of a soil profile with different soil horizons annotated. To cover the variations within each soil horizon, point spectra were measured at least three times within the same soil horizon. In total, 268 spectra were gathered from 16 soil profiles. For some sites, archaeological stratum was not observed on the soil profile, but rather observed at the floor of the pit (for sites 2 and 3). Therefore, in these sites, the soil spectra were also gathered from the floor of the excavated pits.

Collected spectra were first divided by a (white) reference spectrum measured with an ASD Spectralon. Then the continuum removal method (Clark and Roush, 1984) was applied to the spectra. The continuum removal normalizes the reflectance spectra and, therefore, exaggerates the individual absorption features by dividing each spectrum by the corresponding continuum line. Due to an increased instrumental noise observed in the low wavelength region of the soil spectra (Choi, 2018), spectra from 400 to 450 nm were smoothed by a 10 nm Gaussian kernel. The original spectra were collected at intervals of 1 nm (yielding in total 2151 data points from 350 to 2500 nm), but these were re-gridded by selecting data points at ten-nanometer steps (resulting in only 216 data points) in order to be directly comparable to the dataset from the online soil spectral library (Garrity and Bindraban, 2004).

## 3. Modified principal component analysis method

### 3.1. Principal component analysis (PCA)

In soil spectroscopy, PCA is a statistical data reduction method and is a well-known and powerful tool (Friedman et al., 2001; Hotelling, 1933; Jolliffe, 2002; Pearson, 1901) for revealing information in the near infrared region (Martens and Naes, 1984; Stenberg et al., 1995; Wold et al., 1987). It is widely used not only for soil analysis (Knadel et al., 2013; Linker et al., 2005; Reid and Spencer, 2009; Salehi and Zahedi Amiri, 2005; Singh et al., 2011; Viscarra Rossel, 2008), but also for archaeological applications (Aqdus et al., 2008; Doneus et al., 2014; Linderholm et al., 2019; Panishkan et al., 2012; Traviglia, 2006; Wells et al., 2007).

In PCA, a group of soil spectra, the original dataset, is reoriented into a new set of variables called principal components (PC). These PCs depend on the dataset they are generated from and, therefore, the results are not unique properties of the individual samples, but are determined in the context of a larger dataset. The first PC accounts for the greatest variability in the dataset and the second PC accounts for the second greatest variability in the dataset and so on. Therefore, the higher order principal components often represent noise, although they still might represent very rare soil spectral features (Doneus et al., 2014; Traviglia, 2006). Viscarra Rossel et al. (2006) showed that in soil spectroscopy, the first three principal components accounts for approximately 75% of the variation in the data. This indicates that spectroscopic soil properties are represented by only a few characteristic spectral features. A study by Viscarra Rossel et al. (2016), showed that in the cases they examined, the first PC is related to weathered soil mineralogy (iron oxides and kaolinite) and has the strongest positive correlations to silt, inorganic carbon, and iron. Therefore, this paper will only account for the first three principal component values since the first three principal components accounts for more the 97% (Fig. 2) of the variation. The results of this study show this to be an appropriate simplification since very little variation was due to higher-order PCs.

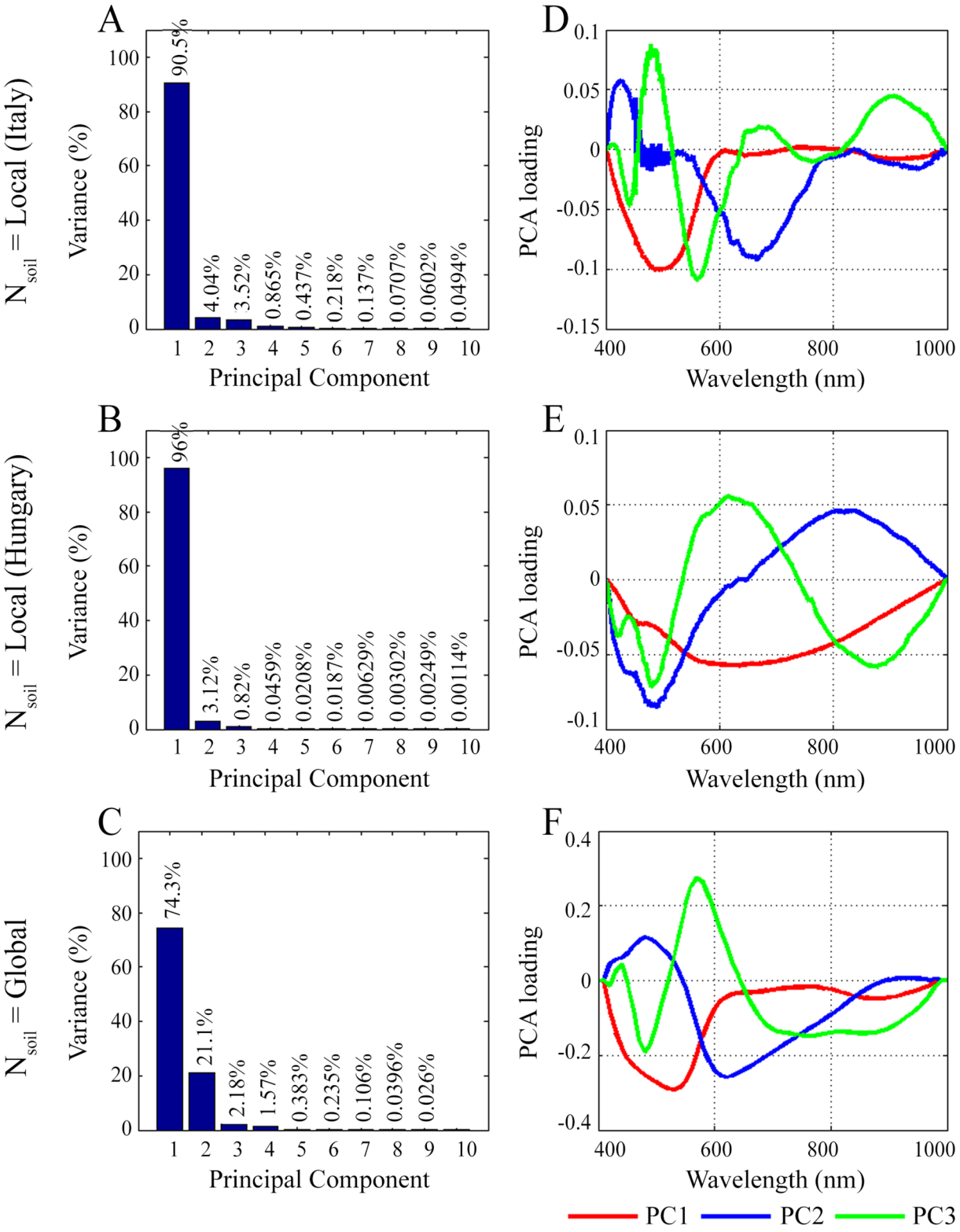


**Fig. 2.** Variance plot (A, B and C) and the first three principal components (D, E and F) for a group of natural soils from Italy (A and D), Hungary (B and E) and global (C and F).

### *3.2. Modified PCA calculation: $N_{soil}$*

Based on the concept of the PCA, this paper introduces a method which further develops the PCA calculation to identify reflectance spectra of buried archaeological remains. The method is based on the hypothesis that all non-archaeological soils in a particular soil landscape, i.e. soils without any archaeological artefacts or strata, have a specific, limited range of spectral signatures and these are mostly represented by the first three principal components. Therefore, any soil spectrum measured in the field should contain spectral characteristics (the first three principal components) of natural soils and, if not, then this spectrum represents an anomalous material, for example an

archaeological material. Based on this hypothesis, one needs to select a group of soil spectra to calculate the first three PCs representing "natural soils". This group of spectra of natural soils will be annotated as $N_{soil}$ in the following.

This paper uses two types of $N_{soil}$: local $N_{soil}$, which represent of spectra of natural soils gathered around the archaeological site (soil spectra gathered in Italy or Hungary), or global $N_{soil}$ which represents soil spectra from the International Soil Reference and Information Centre (ICRAF-ISRIC, 2010). Fig. 2 shows the first three principal components and the variance of local (Italy and Hungary) and global $N_{soil}$. Notice that, although the hypothesis assumes that natural soils have similar spectral behavior, the intensity plots of the local and global $N_{soil}$ illustrate that this is not completely true. The first PC of the Italian $N_{soil}$ and global $N_{soil}$ are similar to each other, but the first PC of the Hungarian $N_{soil}$ shows a rather different spectral feature. Also notice that the first PC of the Hungarian soils represents a rather high variance of 96% indicating that the corresponding soils are very similar to each other, at least in the spectral ranges used, although they are different from those of the other sites. PCs obtained from groups of natural soils will be named natural principal components (*NPC*) in this paper.

### 3.3. Modified PCA calculation: D and R values

After the selection of $N_{soil}$, the next step is to represent the original spectra in terms of the characteristics (*NPCs*) of $N_{soil}$. Thus, the original spectrum, *S*, is recalculated as spectrum *S'* by following equation:

$$S' = S_m + \sum_{i=1}^{n} NT_i * NPC_i \quad (1)$$

Here, $S_m$ is the mean of $N_{soil}$ and $NT_i$ is the weight of the original spectrum calculated by using *NPC*. Since only the first three components are considered, *n* is either 2 or 3.

This recalculated spectrum *S'* contains only the spectral characteristics of the natural soils ($N_{soil}$) and is, thus, similar to the original spectrum *S* only if that spectrum *S* represents a natural soil. The differences between the original ($S_\lambda$) and the recalculated ($S_\lambda'$) spectrum can be described by a so-called D-value, which is calculated using the Euclidean distance.

$$D = \sqrt{\sum_{\lambda} (S_\lambda - S_\lambda')^2} \quad (2)$$

If the difference between the original and recalculated spectrum is small ($D \approx 0$), this indicates that the measured spectrum is similar to, and may represent, a natural soil. However, if the D value is large, then the spectrum more likely represents a non-natural soil, which may be an anthropogenic or specifically an archaeological material. Fig. 3 illustrates the method and shows how a spectrum *S* is changed into *S'* which contains the characteristic information of natural soils. Finally, the ratio, R, between the D value of the unknown sample ($D_{arch}$, since we expect this to be an archaeological material) and the average of those representing natural soils ($D_{nat}$) is calculated.

$$R = \frac{D_{arch}}{D_{nat}} \quad (3)$$

If $D_{arch}$ represents an archaeological material, then the R value should be larger than 1. In the next step we apply this methodology to spectra taken at the study sites to test this hypothesis.

## 4. Results

### 4.1. Soil properties

Table 1 summarizes some basic soil properties between the archaeological and natural soils. The nitrogen content is around 0.1% for all sites, despite whether the spectra represent an archaeological material or natural soil. The pH varies between 7.3 and 7.9. Slight differences are observed for the total carbon content where site 2 has the highest and site 1 has the lowest values. The Hungarian sites have more consistent carbon contents than the Italian site (1.5 vs. 3.7%) which indicates the difference in their origins. One characteristic feature is that, the carbon content tends to be higher for natural soils than for archaeological soils, except for site 1 and site 4 (pit features, for which the slightly high carbon content might be related to due to high fraction of organic matter).

### 4.2. PCA

Principal component analysis (PCA) was applied to the reflectance spectra measured at the different sites to get a first impression on whether the PCA can actually detect spectral features of archaeological materials. The intensity and score plots of the first three principal components of individual archaeological sites are present in Fig. 4. Clear differences between the archaeological materials and natural soils are found at site 1 (prehistoric kitchen formation) and site 4 (an ancient rubbish dump). One interesting point to notice is that in the PC2-PC3 score plot of site 1, there is even a separation of different types of archaeological materials within the site, where burned materials are on the left side of the natural soil cluster (negative PC2 values) and reddish archaeological soils are on the right side of the cluster (positive PC2 values). At this site (site 1), natural soils tend to have PC2 value of approximately 0 indicating that PC2 mainly represents the spectral features of archaeological materials. For sites 2 and 3, some archaeological soils are separated but around half of the archaeological materials are mixed within the natural soil cluster. For site 5, it seems like the PCA method does not work although one could observe a clear color difference between the buried remain and the surrounding soils at this site. This might be related to the reason that the proposed method is not dependent on the soil color (Choi et al., 2015). In addition, the ditch is filled with the yellowish Hungarian loess which may not have large anthropogenic influence and thus more likely to be a natural soil.

The PCA results showed that PCA has the potential to separate archaeological materials from natural soils at sites where there has been a clear chemical alteration (such as burning at site 1 or organic decomposition at site 4).

### 4.3. Modified PCA using local soils

Fig. 5 shows the D and R values of the five archaeological sites when the modified PCA method is applied with the respective local and global $N_{soil}$. Although the first two principal components already account for more than 90% of the variance, the PCA score plots in Fig. 4 (PC2 against PC3 plot of site 1) indicate that the third principal component can also contain useful information. Therefore, results for two cases are shown:

1) Only the first two principal components ($\sum_1^2$ PC) are used for the calculation of D and R.
2) The first three principal components ($\sum_1^3$ PC) are used for the calculation of D and R.

Overall, for most of the study sites, R values are larger than 1, indicating that the method can identify spectral signatures of buried remains. One exception is site 5, for which the R value is smaller than 1 if the first two PCs ($\sum_1^2$ PC) are used. This result could be expected, because for site 5, already the PCA score plot (Fig. 2) indicated that spectra for archeological materials and natural soils were not well separated. However, when $\sum_1^3$ PC is used for site 5, the R value exceeds 1 indicating that, for our purpose, the introduced method works better than the original PCA. All $D_{nat}$ values are below 0.05 indicating that natural soils are very similar for each of the considered sites.

To further illustrate the detailed results of the method, Fig. 6 shows the score plots (PC1 versus PC2) for all sites using local and global $N_{soil}$.

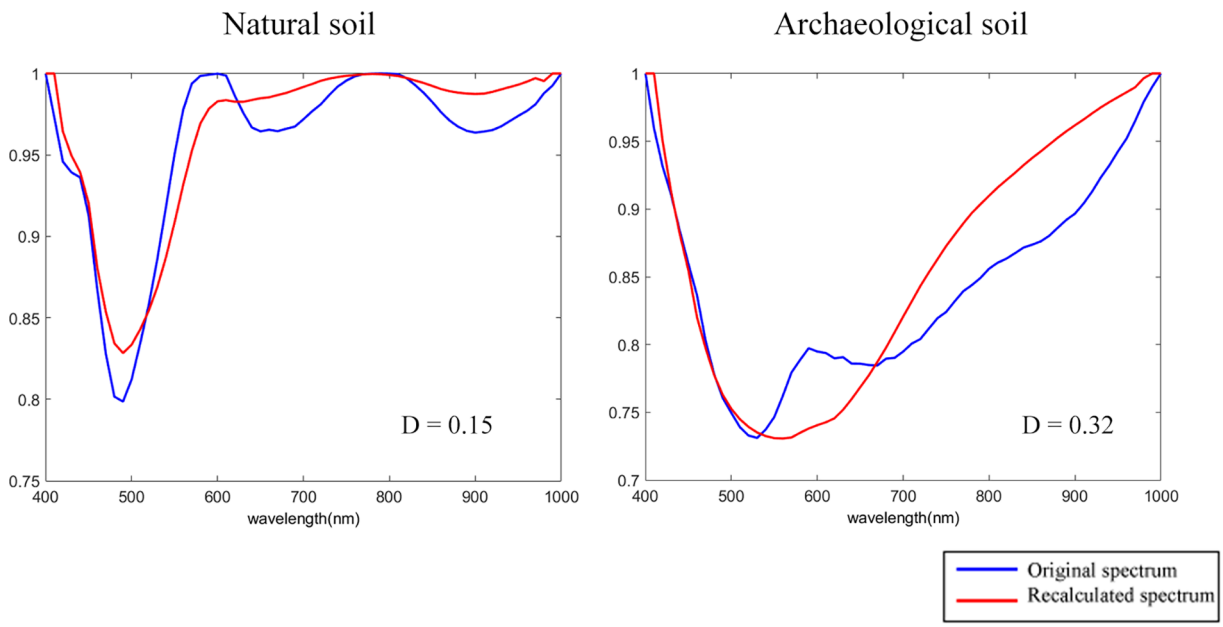


**Fig. 3.** Spectra plot of the original spectrum S and modified spectrum S'. Left image is when S is a natural soil and right image is when S is an archaeological soil (both spectra where chosen from site 1). Notice that some of the absorption features in the archaeological spectrum (around 600 nm) are smoothed out and thus result in larger D values.

**Table 1**
Soil properties of five archaeological sites investigated in Italy (Calabria) and Hungary (Sárvíz Valley). Each archaeological site was identified either by geophysical methods or clear soil marks. Total carbon (C), nitrogen (N), pH and texture of the archaeological soils and non-archaeological soils were averaged for each site. The grey numbers indicate minimum and maximum values. For soil texture, the abbreviations stand for: SCL = sandy clay loam, SL = sandy loam, MS = intermediate coarse sand, SC = sandy clay, Si = silt, SiL = silt loam and L = Loam. N/a = data not available due to not enough soil samples for analysis.

| Country | Italy | Italy | Hungary | Hungary | Hungary |
|---|---|---|---|---|---|
| Site | 1 | 2 | 3 | 4 | 5 |
| | | | Natural soil | | |
| N (%) | 0.1 | 0.1 | 0.1 | 0.1 | 0.1 |
| | 0.1–0.1 | 0.1–0.2 | 0.0–0.2 | 0.1–0.1 | 0.0–0.3 |
| C (%) | 0.7 | 5.2 | 2.3 | 1.5 | 3.7 |
| | 0.4–1.1 | 2.8–7.9 | 0.36–3.6 | 1.5–1.6 | 3.2–4.5 |
| pH | 7.3 | 7.6 | 7.7 | 7.9 | 7.7 |
| | 6.4–7.6 | 7.4–7.7 | 7.6–7.8 | 7.8–8.0 | 7.4–7.9 |
| Texture | SCL/L | SL | SiL | MS/SL | SiL |
| | | | Archaeological soil | | |
| N (%) | 0.1 | 0.1 | 0.1 | 0.1 | 0.1 |
| | 0.1–0.2 | 0.1–0.2 | 0.0–0.1 | 0.1–0.1 | 0.1–0.1 |
| C (%) | 1.6 | 3.7 | 2.2 | 1.7 | 3.1 |
| | 0.7–3.2 | 1.3–5.1 | 0.8–3.2 | 1.7–1.7 | 2.8–3.5 |
| pH | n/a | 7.4 | 7.8 | 7.7 | 7.7 |
| | | 7.4–7.5 | 7.6–7.9 | 7.6–7.8 | 7.6–7.7 |
| Texture | n/a | SiL/SCL/SC/SL | L | MS/SL | L/Si |

In these plots the R value of each spectrum is color coded where high R values are indicated by dark red color. For comparison, in the left column, the same score plots are shown, in which the archeological materials are indicated by red dots, while the data points for natural soils are indicated by open circles. It is found that in most cases, the R values for archaeological spectra are larger than 1. However, it should also be noted that there are also several natural soil spectra with R values larger than 1. Theses natural soil spectra, which have R values larger than 1, are not soil spectra measured below or nearby the archaeological stratum, but are rather soil spectra from natural soil pits which are located around the archaeological remains and thus, are assumed to have not been influenced by any archaeological feature. This indicates that these large R values are not affected by any movement of the soil from the archaeological stratum, but rather represents the variability of the natural soil spectra. For most archaeological materials the R values vary between 3 and 35, depending on the type of archaeological material where soils influenced by a heavy chemical transformation (e.g. effect of fire) tend to yield larger R values.

### 4.4. Modified PCA using global soils

Fig. 5 and Fig. 6 also present the D and R values when global $N_{soil}$ (from the ISRIC spectral library) is used in the calculation. In this case, the $D_{nat}$ values are not as small as for the local $N_{soil}$. Here, the $D_{nat}$ values are mainly larger than 1, but at the same time the $D_{arch}$ values are also larger compared to the local $N_{soil}$ results. These findings indicate that both the spectra of local natural soils and archeological materials have rather large differences to the spectra of the spectral library. Fortunately, the R values are still greater than 1 for most cases indicating the method still works. For example, when global $N_{soil}$ is used the $D_{arch}$ value exceeds 0.5 (for $\sum_1^2$ PC) while the $D_{nat}$ value exceeds 0.3. Therefore, the R value is still larger than 1, indicating that the differences of archaeological materials are larger than those of the natural soil spectra.

Also note that from Fig. 4, the first three principal components of the Italian $N_{soil}$ and global $N_{soil}$ are similar to each other, while the principal components of the Hungarian $N_{soil}$ show rather different features. This finding is also represented by the $D_{nat}$ values (Fig. 5), where the Italian sites (site 1 and 2) have fairly smaller $D_{nat}$ value compared to the Hungarian sites (site 3 to 5).

When the global $N_{soil}$ is used, the R value on average is much smaller than for local $N_{soil}$ but at the same time there are also less false detections of natural soil spectra (natural soil spectra with R values larger than 1, refer to Fig. 6).

### 4.5. Spectral resolution

In this section, it is investigated whether the rather high spectral resolution of the instrument used in this study is actually needed for the identification of archeological materials. For that purpose, the spectral resolution of the measured spectra is systematically degraded to lower

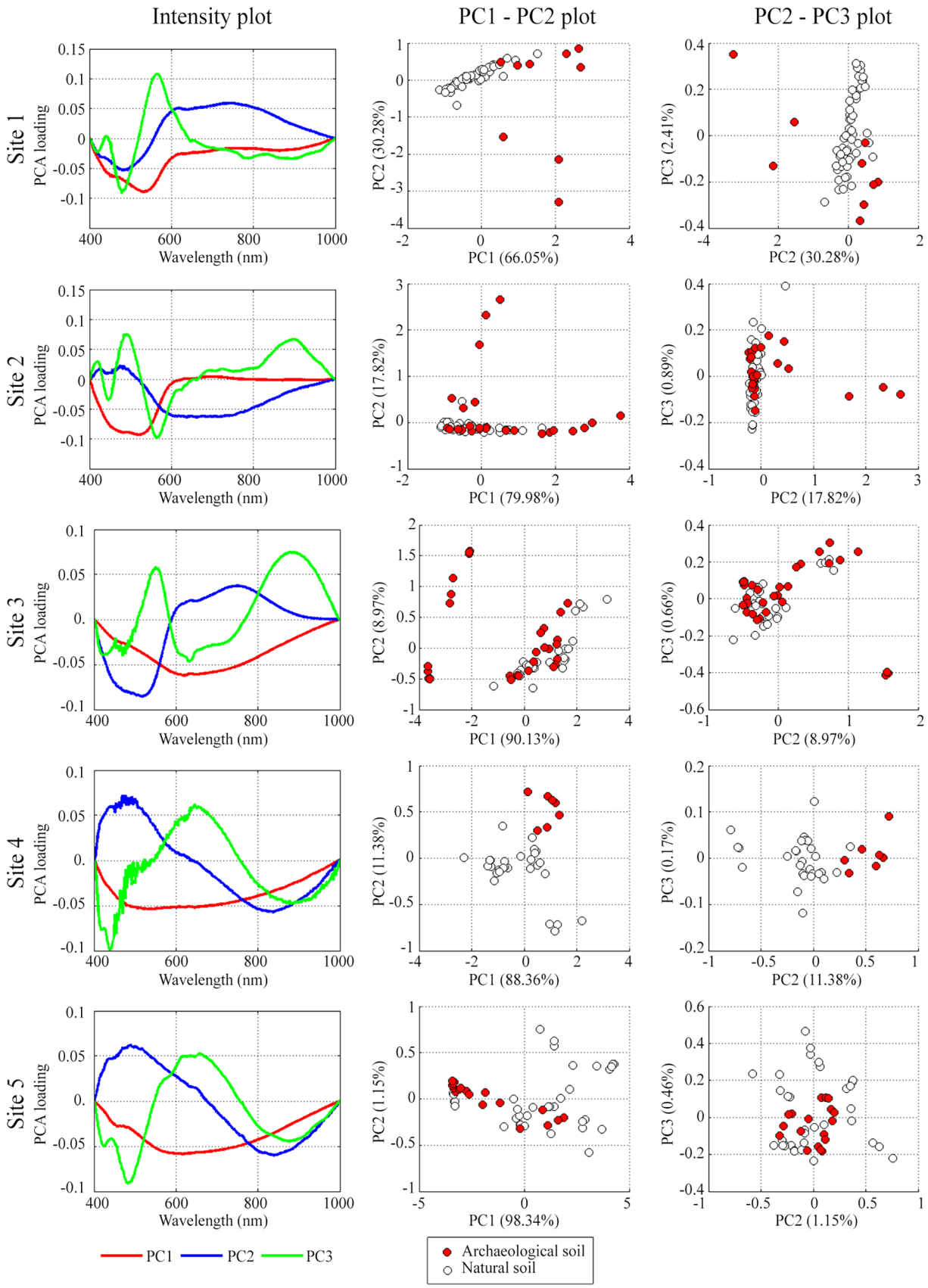


**Fig. 4.** Left: First three principal components for the spectra of all soils. Middle: Scatter plots of the first two principal component scores for archaeological soil (closed circles) and soils surrounding the archaeological site (natural soils, open circles). Right: Scatter plots of the second and third principal component scores.

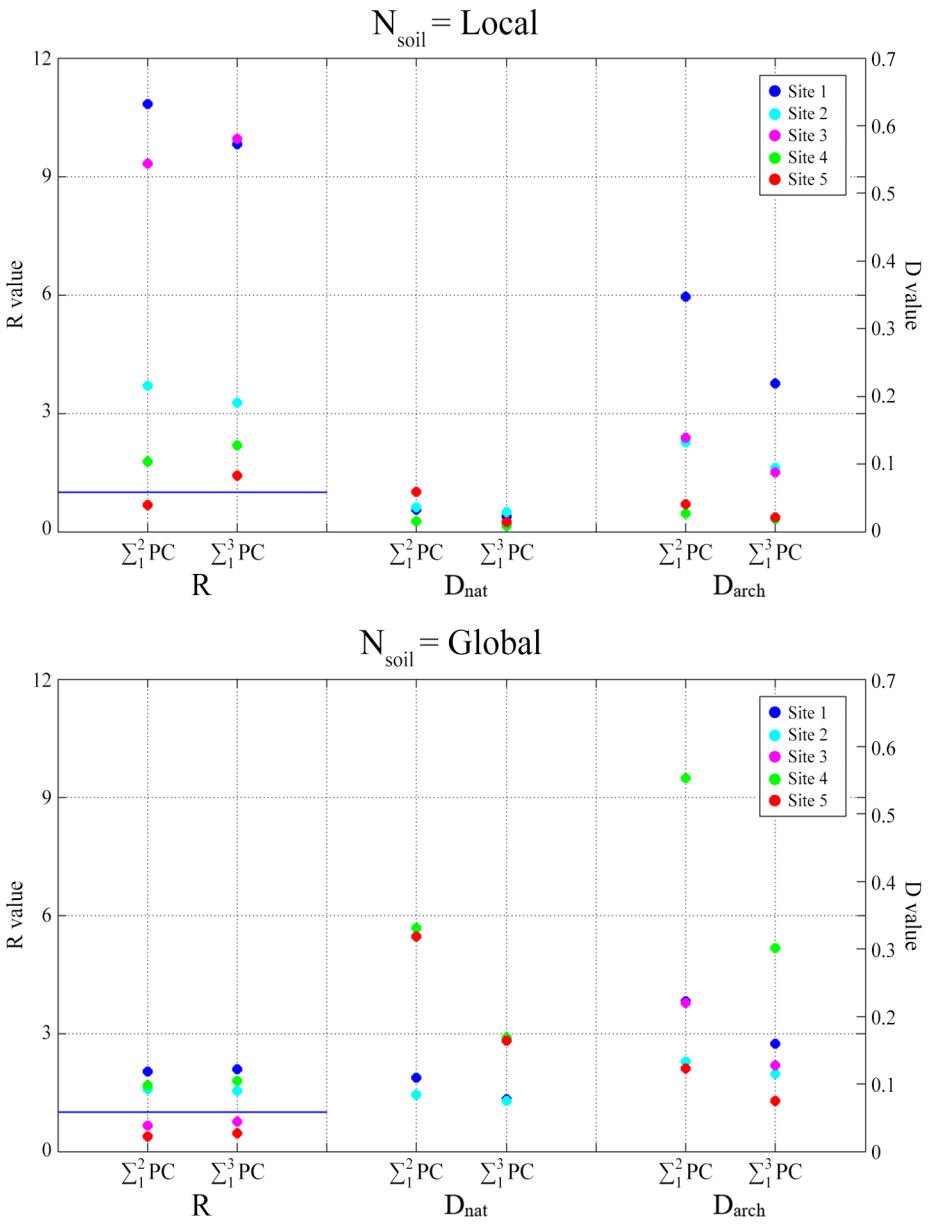


**Fig. 5.** D and R values for the five archaeological sites for local and global $N_{soil}$. The blue line represents a R value of 1. Besides the results for the first two PCs ($\sum_1^2$ PC), also the results for the first three PCs ($\sum_1^3$ PC) are shown. The method distinguishes archaeological spectra for most of the sites when local $N_{soil}$ is used. The ability of the method to distinguish materials of different origins decreases when global $N_{soil}$ is used, but still gives positive values for some of the sites.

spectral resolution by convolution with Gaussian kernels of different widths. Fig. 7 shows an original soil spectrum from site 1 together with smoothed versions of the same spectrum using different Gaussian kernels. After the smoothing the new method is applied in the same way as for the original spectra, and the resulting D and R values are compared with the results for the original spectra.

It is found that the D and R values stay rather stable if the spectra are smoothed by kernels up to 20 nm. For smoothing with kernels ≥ 50 nm, the D and R values either decrease or increase. Interestingly, for some sites, the R values even increase with increasing smoothing kernel. However, for these cases, the $D_{arch}$ values stay rather constant and only the $D_{nat}$ values decrease, which indicates that the increase of the R value is not necessarily an improvement compared to the original spectra.

Overall, the results indicate that the high spectral resolution of the instrument used is not necessary for the application of the method within the range of wavelengths included in this study. In other words, spectral features relevant for the separation of these archaeological materials from natural soils around them are rather broad. Measurements with much lower spectral resolution of up to 20 nm will yield similar results. On the technical side, this finding can have rather important consequences because spectrometers with degraded spectral resolution might use simpler and thus cheaper set-ups. Also, higher optical throughputs and thus higher signal to noise ratios might be established, which in turn can result in shorter integration times.

## 5. Discussion

In this study, five buried archaeological sites were investigated from two environmentally different countries (Italy and Hungary). The sites in Italy contained complex soil compositions and the sites in Hungary had fairly homogenous soils (Hungarian loess). Thus, the initial expectation was that it would be more difficult to identify and classify buried archaeological materials from the sites in Italy. However, the results derived in this paper suggest that the degree of variability of the natural background soils is not problematic as long as the collected natural soil spectra ($N_{soil}$) cover this variability.

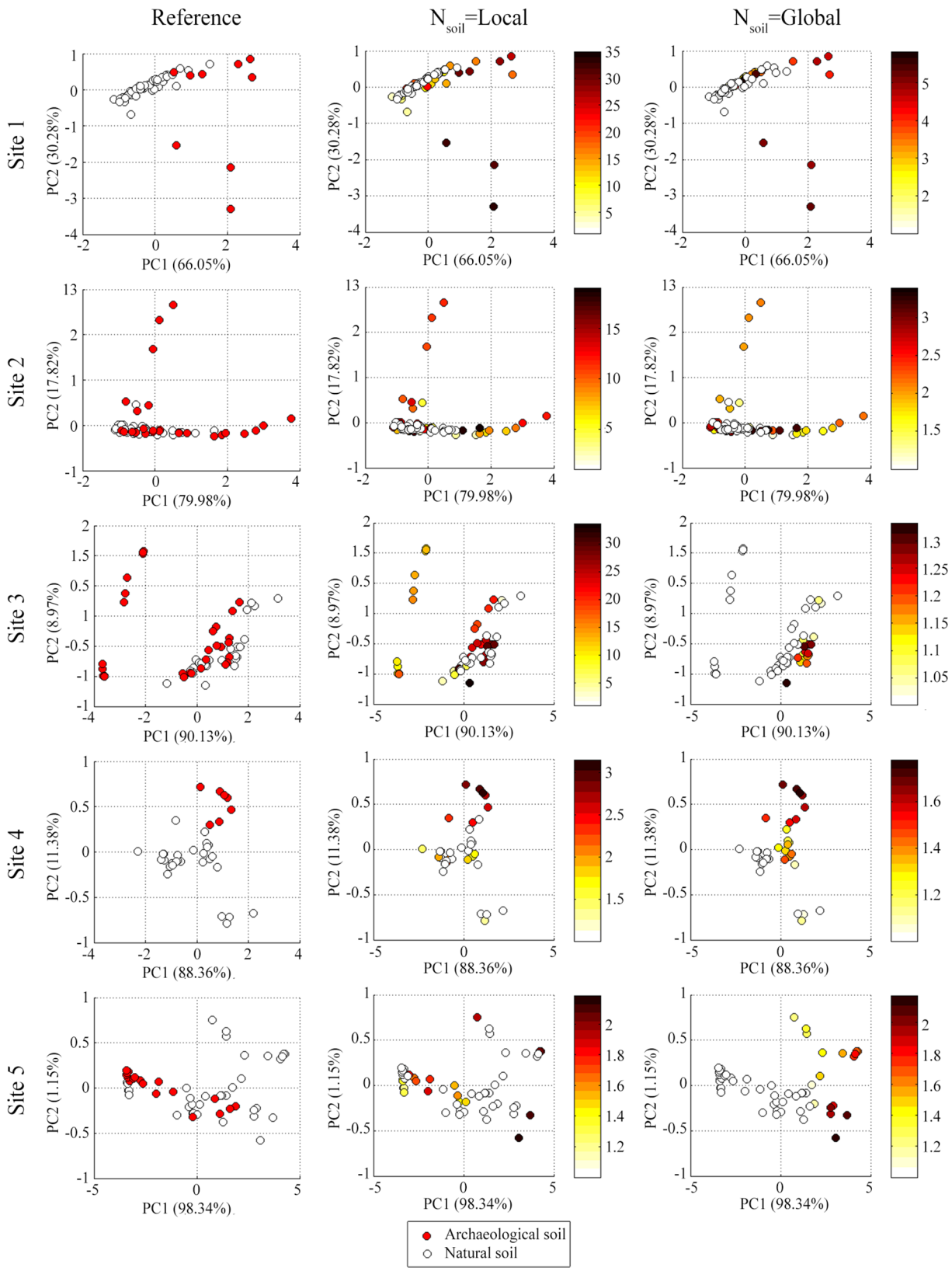


**Fig. 6.** Score plots (PC1 versus PC2 for the PCA based on local $N_{soil}$). Red colors in the left columns indicate archeological material, and open circles indicate natural soils. In the middle and right columns the colors represent the individual R values using either local or global $N_{soil}$. R values below 1 are represented by white (empty) markers and high R values are represented in dark red color.

In addition, the soil properties analyzed through laboratory measurements showed that the soil properties are rather similar between the study sites. Among these results, the carbon content can be linked with the R value results: Sites 1 and 2 were formations including quantities of burnt material where R values were largest and, also for these sites, the difference in the carbon content was large between the

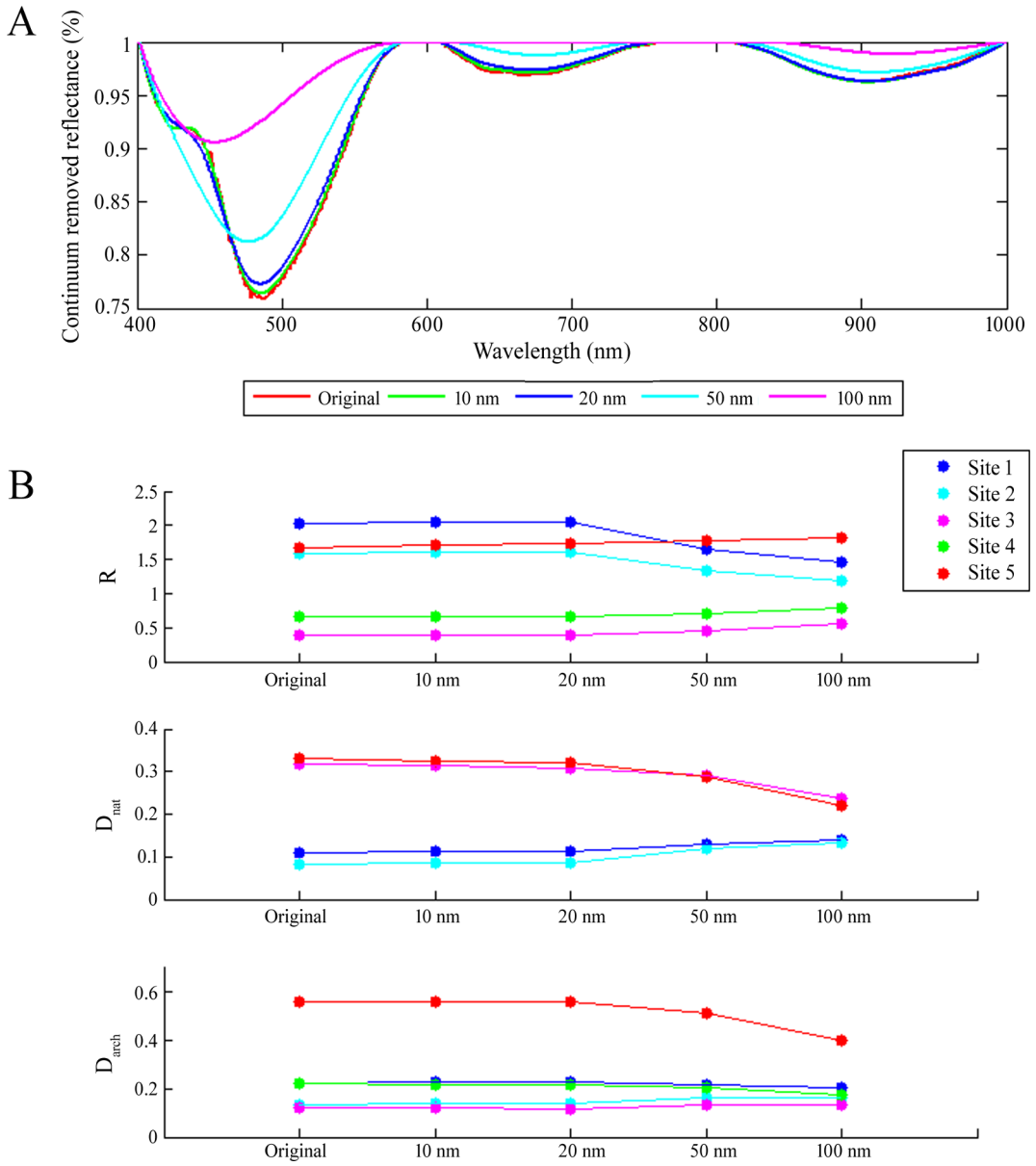


**Fig. 7.** Change in the soil spectra and R values when the spectra are smoothed, for global $N_{soil}$ ($\sum_1^2$ PC). A: Continuum removed reflectance spectrum smoothed by convolution with kernels of 10, 20, 50 and 100 nm (spectrum from site 1). Many small features are smoothed away and the shape of the spectra starts to change as it is smoothed by kernels greater than 50 nm. B: D and R values when spectra are smoothed by convolution of 10, 20, 50 and 100 nm. Degradation of the spectral resolution to values up to about 50 nm does not worsen the results compared to the results for the original spectra.

natural and archaeological soils. However, the link between carbon content and archaeology is clearly complex since site 1 has larger carbon content in archaeological soils but site 2 has higher carbon content in natural soils. The carbon content is also larger at site 4, which could have been the influence of the high organic matter of the pit feature and also a high R value is found for this site. Overall, just by looking at the carbon content, the new method allows a much better distinction between archeological materials and natural soils. This result is similar to the study of Deotare and Kshirsagar (1980) where carbon and nitrogen are recognized in human occupations since they are often subjected to loss by oxidation and leaching.

Soil spectra from the ISRIC spectral library (ICRAF-ISRIC, 2010) can also be used as $N_{soil}$ if there are no natural soil spectra gathered around the archaeological site. However, in this case the R values will be smaller and thus less accurate. This strengthens the point that it is important to gather not only the spectra of the remains but also those of the natural soils in order to reduce the uncertainties. In addition, the results presented emphasize that the R value depends on the type of buried remains.

The introduced method works especially well with materials from burnt deposits, giving R values larger than 3, probably because of the exposure of the materials to fire (Arcenegui et al., 2008). The red soil color of the archaeological stratum observed in site 1 and 2 might also be the result of fire (Matney et al., 2014). Spectra of pit features (site 4) also yield high R values (larger than 1.7), since pit features contain high amounts of organic carbon, nitrogen, or phosphorus compared to the adjacent natural soils (Lauer et al., 2014; Slager and Van de Wetering, 1977). However, for ditch features (sites 3 and 5), depending on what has fallen into the ditch (e.g. collapsed surrounding soil or walls which are still 'natural' soils) the identification might be difficult, despite the color difference to the surrounding natural soils. Such infilling of ditches through natural depositions are mainly slope deposits (Mücher et al., 2018). One important additional factor, in particular on the pit-feature strata, is the probable effect of post-depositional pedogenesis. In the Hungarian sites (sites 3 and 5), in particular, this is likely to

have included the preservation of organic matter and periodic changes in general soil redox state as a result of water fluctuation – which is not likely to have been significant in the much drier Italian sites.

One important point to notice is that, for archaeological applications the spectral resolution can be reduced by a factor 3 to 6 without a significant loss of information. The R value did not change dramatically when the spectra were smoothed by convolution kernels of 10 to 20 nm. This indicates that the broadband features contain the main characteristic differences between natural and archaeological soils. This is an important result, because it provides the possibility to use spectrometers with much lower spectral resolution than the ASD spectrometer and to reduce the integration time. For such spectrometers, either the temporal or spatial resolution (or both) of the measurements can be largely improved. This can even lead to the possibility of performing continuous 1D or 2D imaging measurements and even drone-based spectrometers with reduced acquisition times. Conceptually, this method can be applied to images of spectra collected by other instruments, such as from airborne hyperspectral multispectral images or even satellite images with sufficient spatial resolution where the spectral resolution is not as fine as that of the ground-based spectrometers.

This method is applicable not only to archaeological remains but also to all anthropogenic materials, such as modern materials and soil alterations, on and in the ground. This paper specifically applied the methods to archaeological remains, but the method may be of wider interest because it can be applied to anthropogenic changes in soil spectral characteristics more generally.

## 6. Conclusion

This study presents a modified PCA method to identify spectral signatures of buried archaeological remains among adjacent soils. The introduced method yields a quantitative result by using spectral measurements from a handheld spectrometer in a non-destructive and time efficient way. The method can even be applied to data gathered by a low resolution spectrometer (spectral resolution of 20 nm and spectral range of 400 to 1000 nm) despite the complexity of the background soils. This opens the possibility of performing measurements with short integration times and thus continuous imaging measurements such as drone or airborne measurements.

In this paper the method is successfully applied to five different archaeological sites, but the study also indicated that the effectiveness of the method greatly depends on the type of archaeological remains. Thus, by applying the method to various archaeological sites in different environments the method could be extended and probably be made more specific.

## Acknowledgment

This work was part of the ANAGHLIA (Analysis and ground truthing of hyperspectral and LiDAR images in Archaeology) project and the PhD thesis of Yoon Jung Choi. The PhD study was funded by the Max Planck Institute for Chemistry, Germany (MPIC) and Johannes Gutenberg University Mainz, Germany (Geocycles project). We would like to thank Dr. Steffen Beirle for advise in the method development, Dr. Stibrányi Máté for the Hungarian field campaign and Dr. Martijn van Leusen for the Italian field campaign.

## References

Angelopoulou, T., Tziolas, N., Balafoutis, A., Zalidis, G., Bochtis, D., 2019. Remote sensing techniques for soil organic carbon estimation: a review. Remote Sens. 11 (6), 676. https://doi.org/10.3390/rs11060676.

Aqdus, S.A., Drummond, J., Hanson, W.S., 2008. Discovering archaeological cropmarks: a hyperspectral approach. Int. Archiv. Photogram. Remote Sens. Spatial Inform. Sci. 37, 361–365.

Araújo, S.R., Söderström, M., Eriksson, J., Isendahl, C., Stenborg, P., Demattê, J.M., 2015. Determining soil properties in Amazonian Dark Earths by reflectance spectroscopy. Geoderma 237, 308–317. https://doi.org/10.1016/j.geoderma.2014.09.014.

Arcenegui, V., Guerrero, C., Mataix-Solera, J., Mataix-Beneyto, J., Zornoza, R., Morales, J., Mayoral, A.M., 2008. The presence of ash as an interference factor in the estimation of the maximum temperature reached in burned soils using near-infrared spectroscopy (NIR). Catena 74 (3), 177–184. https://doi.org/10.1016/j.catena.2007.11.004.

Ben-Dor, E., Banin, A., 1995. Near-infrared analysis as a rapid method to simultaneously evaluate several soil properties. Soil Sci. Soc. Am. J. 59 (2), 364–372. https://doi.org/10.2136/sssaj1995.03615995005900020014x.

Ben-Dor, E., Inbar, Y., Chen, Y., 1997. The reflectance spectra of organic matter in the visible near-infrared and short wave infrared region (400–2500 nm) during a controlled decomposition process. Remote Sens. Environ. 61 (1), 1–15. https://doi.org/10.1016/s0034-4257(96)00120-4.

Ben Dor, E., Irons, J.R., Epema, J.F., 1999. Soil reflectance. In: Rencz, A.N., Ryerson, R.A. (Eds.), Manual of Remote Sensing: Remote Sensing for the Earth Sciences. John Wiley & Sons, New York, NY, pp. 111–188.

Ben-Dor, E., Patkin, K., Banin, A., Karnieli, A., 2002. Mapping of several soil properties using DAIS-7915 hyperspectral scanner data-a case study over clayey soils in Israel. Int. J. Remote Sens. 23 (6), 1043–1062. https://doi.org/10.1080/01431160010006962.

Ben-Dor, E., Taylor, R.G., Hill, J., Demattê, J.A.M., Whiting, M.L., Chabrillat, S., Sommer, S., 2008. Imaging spectrometry for soil applications. Adv. Agron. 97, 321–392. https://doi.org/10.1016/s0065-2113(07)00008-9.

Buck, P.E., Sabol, D.E., Gillespie, A.R., 2003. Sub-pixel artifact detection using remote sensing. J. Archaeol. Sci. 30 (8), 973–989. https://doi.org/10.1016/S0305-4403(02)00284-4.

Deotare, B.C., Kshirsagar, A.A., 1980. Phosphorus contents of some archaeological and non-archaeological deposits in India. Bull. Deccan College Res. Inst. 39, 27–29.

Choi, Y. J. (2018) Development of a spectroscopic method to identify archaeological remains and soils using reflectance spectra in the visible to near infrared region. Dissertation, Johannes Gutenberg University Mainz.

Choi, Y.J., Lampel, L., Jordan, D., Fiedler, S., Wagner, T., 2015. Principal component analysis (PCA) of buried archaeological remains by VIS-NIR spectroscopy. Archaeologia Polona 53, 412–415.

Clark, R.N., King, T.V., Klejwa, M., Swayze, G.A., Vergo, N., 1990. High spectral resolution reflectance spectroscopy of minerals. J. Geophys. Res. Solid Earth 95 (B8), 12653–12680. https://doi.org/10.1029/jb095ib08p12653.

Clark, R.N., Roush, T.L., 1984. Reflectance spectroscopy: Quantitative analysis techniques for remote sensing applications. J. Geophys. Res. Solid Earth 89 (B7), 6329–6340. https://doi.org/10.1029/jb089ib07p06329.

Clark, R.N., Swayze, G.A., Livo, K.E., Kokaly, R.F., Sutley, S.J., Dalton, J.B., McDougal, R.R., Gent, C.A., 2003. Imaging spectroscopy: earth and planetary remote sensing with the USGS Tetracorder and expert systems. J. Geophys. Res. Planets 108 (E12). https://doi.org/10.1029/2002je001847.

Cook, S.F., Heizer, R.F., 1964. Studies on the Chemical Analysis of Archaeological Sites. University of California Publications in Anthropology, pp. 2.

Doneus, M., Verhoeven, G., Atzberger, C., Wess, M., Ruš, M., 2014. New ways to extract archaeological information from hyperspectral pixels. J. Archaeol. Sci. 52, 84–96. https://doi.org/10.1016/j.jas.2014.08.023.

Eckmeier, E., Gerlach, R., 2012. Characterization of archaeological soils and sediments using VIS spectroscopy. J. Ancient Stud. 3, 285–290.

Eidt, R.C., 1984. Advances in Abandoned Settlement Analysis: Application to Prehistoric Anthrosols in Colombia, South America. Center for Latin America, University of Wisconsin-Milwaukee, Milwaukee, WI.

Friedman, J., Hastie, T., Tibshirani, R., 2001. The Elements of Statistical Learning Vol. 1, No. 10 Springer series in statistics, New York.

Garrity, D., Bindraban, P., 2004. A globally distributed soil spectral library visible near infrared diffuse reflectance spectra. In: ICRAF (World Agroforestry Centre)/ISRIC (World Soil Information) Spectral Library: Nairobi, Kenya.

Greweling, T., 1962. Plant tissue analysis, an extraction procedure for the determination of total calcium, magnesium, and potassium in plant tissue. J. Agric. Food. Chem. 10 (2), 138–140. https://doi.org/10.1021/jf60120a016.

Grøn, O., Palmer, S., Stylegar, F.A., Esbensen, K., Kucheryavski, S., Aase, S., 2011. Interpretation of archaeological small-scale features in spectral images. J. Archaeol. Sci. 38 (9), 2024–2030. https://doi.org/10.1016/j.jas.2009.11.023.

Hao, X., Chang, C., 2003. Does long-term heavy cattle manure application increase salinity of a clay loam soil in semi-arid southern Alberta? Agric. Ecosyst. Environ. 94 (1), 89–103. https://doi.org/10.1016/s0167-8809(02)00008-7.

Haslam, R., Tibbett, M., 2004. Sampling and analyzing metals in soils for archaeological prospection: a critique. Geoarchaeol. Int. J. 19 (8), 731–751. https://doi.org/10.1002/gea.20022.

Hong, Y., Yu, L., Chen, Y., Liu, Y., Liu, Y., Liu, Y., Cheng, H., 2018. Prediction of soil organic matter by VIS–NIR spectroscopy using normalized soil moisture index as a proxy of soil moisture. Remote Sens. 10, 28. https://doi.org/10.3390/rs10010028.

Hotelling, H., 1933. Analysis of a complex of statistical variables into principal components. J. Educ. Psychol. 24 (6), 417. https://doi.org/10.1037/h0070888.

ICRAF-ISRIC. (2010). A Globally Distributed Soil Spectral Library: Visible Near Infrared Diffuse Reflectance Spectra. World Agroforestry Centre (ICRAF) and ISRIC - World Soil Information. Retrieved from http://www.africasoils.net/afsis_files/ICRAF-ISRICSoilVNIRSpectralLibrary.pdf.

Jahn, R., Blume, H. P., Asio, V. B., Spaargaren, O., & Schad, P. (2006). Guidelines for soil description. FAO.

Jolliffe, I.T., 2002. Springer series in statistics. Principal Component Anal. 29. https://doi.org/10.1007/b98835.

Knadel, M., Viscarra Rossel, R.A., Deng, F., Thomsen, A., Greve, M.H., 2013. Visible–near infrared spectra as a proxy for topsoil texture and glacial boundaries. Soil Sci. Soc.

Am. J. 77 (2), 568–579. https://doi.org/10.2136/sssaj2012.0093.
Lauer, F., Prost, K., Gerlach, R., Pätzold, S., Wolf, M., Urmersbach, S., Amelung, W., et al., 2014. Organic fertilization and sufficient nutrient status in prehistoric agriculture?–indications from multi-proxy analyses of archaeological topsoil relicts. PloS one 9 (9), e106244. https://doi.org/10.1371/journal.pone.0106244.
Linderholm, J., Geladi, P., Gorretta, N., Bendoula, R., Gobrecht, A., 2019. Near infrared and hyperspectral studies of archaeological stratigraphy and statistical considerations. Geoarchaeology 34 (3), 311–321. https://doi.org/10.1002/gea.21731.
Linker, R., Shmulevich, I., Kenny, A., Shaviv, A., 2005. Soil identification and chemometrics for direct determination of nitrate in soils using FTIR-ATR mid-infrared spectroscopy. Chemosphere 61 (5), 652–658. https://doi.org/10.1016/j.chemosphere.2005.03.034.
Liu, W., Baret, F., Gu, X., Zhang, B., Tong, Q., Zheng, L., 2003. Evaluation of methods for soil surface moisture estimation from reflectance data. Int. J. Remote Sens. 24 (10), 2069–2083. https://doi.org/10.1080/01431160210163155.
Maly, P., Zamansky, V., Ho, L., Payne, R., 1999. Alternative fuel reburning. Fuel 78 (3), 327–334. https://doi.org/10.1016/s0016-2361(98)00161-6.
Martens, H., & Naes, T. (1984). Multivariate calibration. In Chemometrics. Springer, Dordrecht.
Matney, T., Barrett, L.R., Dawadi, M.B., Maki, D., Maxton, C., Perry, D.S., Roper, D.C., Somers, L., Whitman, L.G., 2014. In situ shallow subsurface reflectance spectroscopy of archaeological soils and features: a case-study of two Native American settlement sites in Kansas. J. Archaeol. Sci. 43, 315–324. https://doi.org/10.1016/j.jas.2013.11.027.
Middleton, W.D., Price, D.T., 1996. Identification of activity areas by multi-element characterization of sediments from modern and archaeological house floors using inductively coupled plasma-atomic emission spectroscopy. J. Archaeol. Sci. 23 (5), 673–687. https://doi.org/10.1006/jasc.1996.0064.
Mücher, H., van Steijn, H., & Kwaad, F. (2018). Colluvial and mass wasting deposits. In (?) Interpretation of micromorphological features of soils and regoliths (pp. 21-36). Elsevier. https://doi.org/10.1016/b978-0-444-63522-8.00002-4.
Nocita, M., Stevens, A., van Wesemael, B., Aitkenhead, M., Bachmann, M., Barthès, B., Dor, E.B., Brown, D.J., Clairotte, M., Csorba, A., Dardenne, P., 2015. Soil spectroscopy: an alternative to wet chemistry for soil monitoring. Adv. Agron. 132, 139–159. https://doi.org/10.1016/bs.agron.2015.02.002.
Oonk, S., Slomp, C.P., Huisman, D.J., 2009. Geochemistry as an aid in archaeological prospection and site interpretation: current issues and research directions. Archaeol. Prospection 16 (1), 35–51. https://doi.org/10.1002/arp.344.
Ottaway, J.H., Matthews, M.R., 1988. Trace element analysis of soil samples from a stratified archaeological site. Environ. Geochem. Health 10 (3–4), 105–112. https://doi.org/10.1007/bf01758678.
Panishkan, K., Swangjang, K., Sanmanee, N., Sungthong, D., 2012. Principal component analysis for the characterization in the application of some soil properties. Int. J. Environ. Ecol. Eng. 6 (5), 279–281.
Pearson, K. (1901). LIII. On lines and planes of closest fit to systems of points in space. The London, Edinburgh, and Dublin Philosophical Magazine and Journal of Science, 2(11), 559-572. https://doi.org/10.1080/14786440109462720.
Reid, M.K., Spencer, K.L., 2009. Use of principal components analysis (PCA) on estuarine sediment datasets: the effect of data pre-treatment. Environ. Pollut. 157 (8–9), 2275–2281. https://doi.org/10.1016/j.envpol.2009.03.033.
Salehi, A., Zahedi Amiri, G., 2005. Study of physical and chemical soil properties variations using principal component analysis method in the forest, North of Iran. Caspian J. Environ. Sci. 3 (2), 131–137.
Schmid, T., Koch, M., DiBlasi, M., Hagos, M., 2008. Spatial and spectral analysis of soil surface properties for an archaeological area in Aksum, Ethiopia, applying high and medium resolution data. Catena 75 (1), 93–101. https://doi.org/10.1016/j.catena.2008.04.008.
Singh, V., Agrawal, H.M., Joshi, G.C., Sudershan, M., Sinha, A.K., 2011. Elemental profile of agricultural soil by the EDXRF technique and use of the Principal Component Analysis (PCA) method to interpret the complex data. Appl. Radiat. Isot. 69 (7), 969–974. https://doi.org/10.1016/j.apradiso.2011.01.025.
Slager, S., Van de Wetering, H.T.J., 1977. Soil formation in archaeological pits and adjacent loess soils in Southern Germany. J. Archaeolog. Sci. 4 (3), 259–267. https://doi.org/10.1016/0305-4403(77)90093-0.
Soriano-Disla, J.M., Janik, L.J., Viscarra Rossel, R.A., Macdonald, L.M., McLaughlin, M.J., 2014. The performance of visible, near-, and mid-infrared reflectance spectroscopy for prediction of soil physical, chemical, and biological properties. Appl. Spectrosc. Rev. 49 (2), 139–186. https://doi.org/10.1080/05704928.2013.811081.
Stenberg, B.O., Nordkvist, E., Salomonsson, L., 1995. Use of near infrared reflectance spectra of soils for objective selection of samples. Soil Sci. 159 (2), 109–114. https://doi.org/10.1097/00010694-199502000-00005.
Stenberg, B., Viscarra Rossel, R.A., Mouazen, A.M., Wetterlind, J., 2010. Visible and near infrared spectroscopy in soil science. Adv. Agron. 107, 163–215. https://doi.org/10.1016/s0065-2113(10)07005-7.
Traviglia, A., 2006. Archaeological usability of hyperspectral images: Successes and failures of image processing techniques. BAR International Series 1568, 123.
Van Reeuwijk, L. P. (2002). Technical Paper 09: Procedures for Soil Analysis (6th Edition). Retrieved from https://www.isric.org/documents/document-type/technical-paper-09-procedures-soil-analysis-6th-edition.
Viscarra Rossel, R.A., McGlynn, R.N., McBratney, A.B., 2006. Determining the composition of mineral-organic mixes using UV–vis–NIR diffuse reflectance spectroscopy. Geoderma 137 (1–2), 70–82. https://doi.org/10.1016/j.geoderma.2006.07.004.
Viscarra Rossel, R.A., 2008. ParLeS: Software for chemometric analysis of spectroscopic data. Chemometr. Intell. Lab. Syst. 90 (1), 72–83. https://doi.org/10.1016/j.chemolab.2007.06.006.
Viscarra Rossel, R.A., Behrens, T., 2010. Using data mining to model and interpret soil diffuse reflectance spectra. Geoderma 158 (1–2), 46–54. https://doi.org/10.1016/j.geoderma.2009.12.025.
Viscarra Rossel, R.A., Cattle, S.R., Ortega, A., Fouad, Y., 2009. In situ measurements of soil colour, mineral composition and clay content by vis–NIR spectroscopy. Geoderma 150 (3–4), 253–266. https://doi.org/10.1016/j.geoderma.2009.01.025.
Viscarra Rossel, R.A., Chappell, A., De Caritat, P., McKenzie, N.J., 2011. On the soil information content of visible–near infrared reflectance spectra. Eur. J. Soil Sci. 62 (3), 442–453. https://doi.org/10.1111/j.1365-2389.2011.01372.x.
Viscarra Rossel, R.A., Behrens, T., Ben-Dor, E., Brown, D.J., Demattê, J.A.M., Shepherd, K.D., Aïchi, H., 2016. A global spectral library to characterize the world's soil. Earth Sci. Rev. 155, 198–230. https://doi.org/10.1016/j.earscirev.2016.01.012.
Wells, E. C., Novotny, C., & Hawken, J. R. (2007). Quantitative modeling of soil chemical data from inductively coupled plasma—optical emission spectroscopy reveals evidence for cooking and eating in ancient Mesoamerican plazas. https://doi.org/10.1021/bk-2007-0968.ch011.
Wetterlind, J., Stenberg, B., Rossel, R.A.V., 2013. Soil analysis using visible and near infrared spectroscopy. In: Plant Mineral Nutrients. Humana Press, Totowa, NJ, pp. 95–107. https://doi.org/10.1007/978-1-62703-152-3_6.
Wold, S., Esbensen, K., Geladi, P., 1987. Principal component analysis. Chemometrics and Intelligent Laboratory Systems 2 (1–3), 37–52. https://doi.org/10.1016/0169-7439(87)80084-9.